If God lived on earth, people would break his windows.
YIDDISH PROVERB

16

Spontaneous Symmetry Breakdown

In the perturbation expansion developed in Chapter 10, the classical ground state carries no field. The associated vacuum state is called *normal*, since it is invariant under all symmetry transformations of the action. There are many physical systems where this is not true. As an example, we shall discuss here the ϕ^4-theory with N components $\phi_1, \ldots, \phi_N$ coupled in an O(N)-symmetric way.

16.1 Scalar O(N)-Symmetric ϕ^4-Theory

The relevant Lagrangian reads

$$\mathcal{L} = \frac{1}{2}\left(\partial\phi_a\right)^2 - \frac{m^2}{2}\phi_a^2 - \frac{g}{4}\left(\phi_a^2\right)^2. \tag{16.1}$$

It is invariant under all N-dimensional rotations of its components

$$\phi_a \to R_{ab}\phi_b, \tag{16.2}$$

which conserve the length of the field vector $\phi \equiv (\phi_a)$,

$$|\phi| = \sqrt{\phi_a^2}. \tag{16.3}$$

The perturbation expansion of the ϕ^4-theory discussed in Chapters 10 and 11 was based on a Taylor expansion of the total generating functional

$$Z[j] = e^{-i(g/4)\int_{-\infty}^{\infty} dt[-i\delta/\delta j(x)]^4} Z_0[j] \tag{16.4}$$

in powers of the interaction g, where $Z_0[j]$ is the generating functional of the free-field theory with a Lagrangian

$$\mathcal{L}_0 = \frac{1}{2}\left(\partial\phi_a\right)^2 - \frac{m^2}{2}\phi_a^2. \tag{16.5}$$

This expansion makes sense only for a positive square mass m^2. Assuming a positive coupling constant g, the classical field potential

$$v(\phi_a) = \frac{m^2}{2}\phi_a^2 + \frac{g}{4}\left(\phi_a^2\right)^2 \tag{16.6}$$

has a minimum at the O(N)-symmetric field configuration $\phi_a = \phi_a^0 = 0$. Only in this case can the perturbation expansion of the second-quantized field theory proceed around the free-field theory described by $\mathcal{L}_0$.

A non-trivial and physically very important situation is, however, described by the case $m^2 < 0$ (at $g > 0$). Then the classical field configuration minimizing $\mathcal{L}$ is given by a nonzero field

$$\phi_a^0 \neq 0. \tag{16.7}$$

This happens in various many-body systems, where field theories of the type (16.1) are used to describe orientational properties of materials, for instance the direction of magnetization. In that case $n = 3$, and the vector (ϕ_1, ϕ_2, ϕ_3) is identified with the local size and orientation of the local magnetization. The generating functional

$$Z[j] = \int \mathcal{D}\phi e^{i\int dx[\mathcal{L}(\phi,\partial\phi)+j_a\phi_a]} \tag{16.8}$$

can serve to understand the fluctuation phenomena in such systems. When comparing theory and experiment it turns out that there is usually a certain temperature T_c, above which the system can be described via the perturbation expansion given in the last chapter. As the temperature is lowered toward T_c, fluctuations increase drastically. This can be accounted for in field theory based on (16.1) by letting the mass parameter be temperature dependent such that m^2 vanishes for some temperature $T = T_c^{\rm MF}$, say

$$m^2 = \mu^2 \left(\frac{T}{T_c^{\rm MF}} - 1 \right) \equiv \mu^2 \tau, \tag{16.9}$$

where μ is some mass scale. The temperature $T = T_c^{\rm MF}$ carries a superscript MF to indicate that this is the place where the *bare mass* changes sign, and the mean-field approximation has its phase transition. The fluctuations will shift this temperature downwards, making the true critical temperature T_c smaller than T_c. In the low-temperature phase, the direction of the spin vectors ϕ_a is no more random, but the system settles at a specific non-zero expectation value of the field which we denoted before as

$$\Phi_a \equiv \langle 0|\phi_a|0\rangle. \tag{16.10}$$

Take, for example, a magnetic system which can acquire a certain spontaneous magnetization. The existence of a nonzero expectation value (16.10) introduces a new qualitative feature into the theory. The ground state no longer has the symmetry which was contained in the action. A rotation O(N) changes the direction of the ground state just as a magnet can be rotated in space. One speaks of a *spontaneous breakdown* of the original symmetry of the action.

The perturbative calculation order by order cannot account for this feature since, as we have seen, the evenness of the ϕ^4-interaction prevents the existence of any odd-point function. The effect must therefore be due to a non-perturbative mechanism.

It is gratifying to note that this does not prevent us from giving a theoretical explanation of this phenomenon using perturbation-theoretic techniques. In fact, the effective action that was calculated in the proceeding chapters with perturbative techniques is the ideal tool for this purpose. Note that whatever symmetry is carried by the action $\mathcal{A}[\phi_a]$, this will also wind up in the effective action $\Gamma[\Phi_a]$. Indeed, if $\mathcal{A}[\phi_a]$ does not change under the transformation (16.2), then $W[j_a]$ is invariant under $j_a \to R_{ab} j_b$. Thus the field expectation value $\Phi_a \equiv \delta W/\delta j_a$ transforms according to the same law as the field ϕ_a itself, and $\Gamma[\Phi_a] = W[j_a] - j_a \Phi_a$ will also be invariant.

This statement is obvious at the lowest-order approximation to the effective action which is equal to the classical action $\mathcal{A}[\phi_a]$ taken at Φ_a:

$$\Gamma[\Phi_a] \approx \mathcal{A}[\Phi_a]. \tag{16.11}$$

At a constant field expectation Φ_a, this determines the effective potential

$$\Gamma[\Phi_a] = -V v(\Phi_a), \tag{16.12}$$

where $V = d^D x$ is the spacetime volume. For the Lagrange density (16.1), the effective potential is

$$v(\Phi_a) = \frac{1}{2} m^2 \Phi_a^2 + \frac{g}{4} \left(\Phi_a^2\right)^2. \tag{16.13}$$

Already at this lowest approximation, the effective action is capable of describing a spontaneous symmetry breakdown. As long as $m^2 > 0$, this has an O(N)-symmetric minimum at a single field point, the origin $\Phi_a = 0$. But if m^2 is lowered and becomes smaller than zero, the origin becomes unstable and the potential looks as shown in Fig. 16.1. The O(N)-symmetry of the potential gives rise to an infinitely degenerate minimum characterized by a fixed length of the field vector Φ_a:

$$|\mathbf{\Phi}^0| \equiv \sqrt{\Phi_a^{0\,2}} = \sqrt{\frac{-m^2}{g}}. \tag{16.14}$$

The direction of this minimum in field space can be changed arbitrarily by an O(N)-rotation without changing the energy.

The length scale over which the fluctuations take place is given by the mass term as

$$\xi = m^{-1} = \mu^{-1} \tau^{-1/2}. \tag{16.15}$$

Experimentally one finds the slightly different result

$$\xi = \mu^{-1} \tau^{-\nu}, \tag{16.16}$$

and the power ν is the *critical exponent* or *critical index* of the temperature dependence of the coherence length. In mean-field approximation to (16.10), where β is equal to 1/2. The system is unstable at the origin. Small fluctuations which are

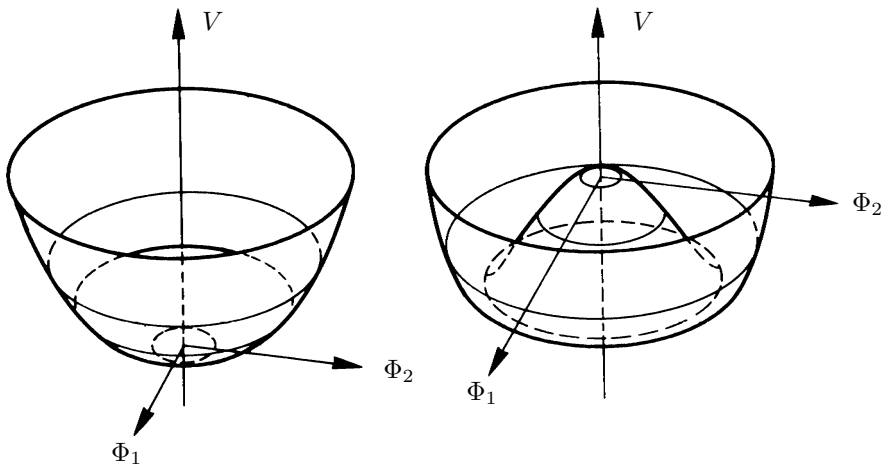

FIGURE 16.1 Effective potential of the ϕ^4-theory for $N = 2$ in mean-field approxmation. It is plotted for $m^2 > 0$ and $m^2 < 0$, corresponding to temperatures above and below the critical temperature, respectively.

neglected within the present classical approximation will drive the field down to a new minimum at Φ_0. The non-perturbative aspect of the solution manifests itself in the power $1/\sqrt{g}$ appearing even at the level of no fluctuations.

Note how the symmetry is spontaneously broken: The system has now many directions to choose from, since there exists an entire surface of an O(N)-sphere, the so-called O(N)-shell, of minimal energy. It is pictured as a circle in Fig. 16.1. One says that for $m^2 < 0$, the vacuum is infinitely degenerate. As soon as Φ_a has made its directional choice, the ground state has lost its symmetry, which is said to be *spontaneously broken*.

From (16.14) we can calculate how the strength of the magnetization varies with temperature using (16.9):

$$|\mathbf{\Phi}^0| = \frac{\mu}{\sqrt{g}}\sqrt{-\tau} = \frac{\mu}{\sqrt{g}}\sqrt{1 - \frac{T}{T_c^{\rm MF}}}. \tag{16.17}$$

Experimentally, one finds a power law slightly different from this:

$$|\mathbf{\Phi}^0| \propto (-\tau)^\beta, \tag{16.18}$$

where the power β is the *critical exponent* or *critical index* of the temperature behavior of the magnetic field. The data lie quite close to the mean-field approximation (16.17), where β has a value $\beta \approx 1/2$ with the plot shown in Fig. 16.2.

The deviation of ν and β from 1/2 is due to fluctuations. In Section 20.8 we shall derive the deviation from 1/2. It will emerge from an expansion of a general scaling relation to be discussed in the section leading to Eq. (20.174). Anticipating

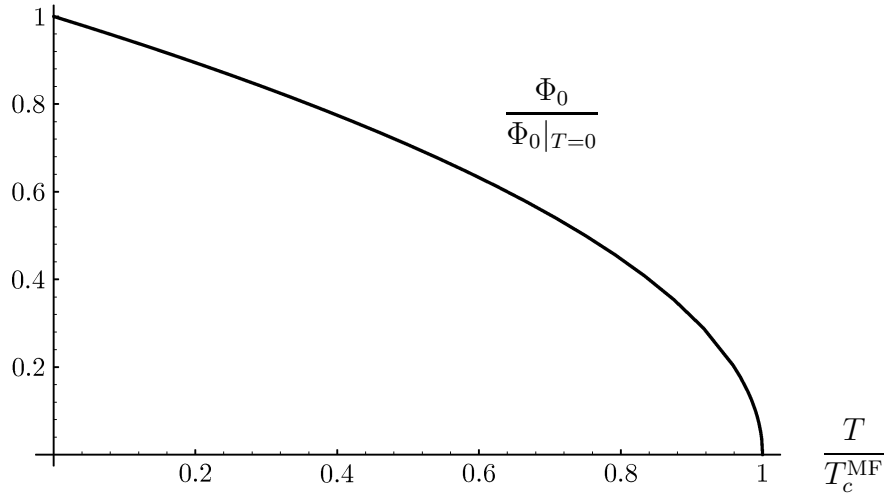

FIGURE 16.2 Magnetization Φ_0 in mean-field approximation as a function of the temperature ratio $T/T_c^{\rm MF}$.

the result for the effective potential $v(\Phi_a)$, we shall find that it depends on $\Phi \equiv \sqrt{\Phi_a^2}$ like

$$v(\Phi_a) = \frac{g^*}{4}\Phi^\delta \left(1 + \text{const} \times \xi^{-\omega}\Phi^{-2\omega/(D-2+\eta)} + \dots\right), \tag{16.19}$$

where for $N = 2$, the critical exponents are $\delta = (D + 2 - \eta)/(D - 2 + \eta) \approx 4.7$, $\eta \approx 0.033$, $\nu \approx 2/3$, $\omega \approx 0.8$.

The expansion (16.19) is derived for positive m^2. What can we say about $m^2 < 0$? Looking at the original one-loop formula we see that the whole effective action can be continued analytically to negative m^2 as long as Φ^2 is kept nonzero, so that

$$m^2 + \frac{g}{2}\Phi^{0\,2} > 0. \tag{16.20}$$

But this is too close to the new minimum which, with the normalization of the coupling used there implying $g_{\rm old} = 3! g_{\rm new}$, was at

$$\Phi^{0\,2} = -\frac{m^2}{g}3! \tag{16.21}$$

such that $m^2 + g\Phi^2/2 = -2m^2 > 0$. Moreover, the full loop expansion formula to all orders can be calculated for Φ close to this minimum since all propagators $\mathcal{D} = i/\left(-\partial^2 - m^2 - g\Phi^2/2\right)$ correspond to particles with a proper positive mass term.

Note that the renormalization procedure is well-defined order by order in the coupling constant g. The same counter terms which made the results finite above

T_c^{MF}, keep the results finite below T_c^{MF}. The only point to watch out is that the Φ never drops below a certain critical value

$$\Phi^2 < \frac{1}{3}\Phi^{02} = -2\frac{m^2}{g}, \tag{16.22}$$

at which place logarithms pick up negative arguments and give rise to imaginary parts. Thus, as long as we avoid the critical value (16.22) we may use (16.19) also for $m^2 < 0,\ T < T_c^{\mathrm{MF}}$. Actually, that result was only derived for a one-component Φ-field. But it can easily be shown that the same form remains valid also for the O(N)-field Φ_a, except with slightly different critical exponents β and γ.

We may now use the expansion (16.19) for the same discussion as before, and find a vacuum expectation below T_c^{MF}:

$$|\mathbf{\Phi}^0| = \left(-\frac{m^2}{g}\right)^{\beta} = (-\tau)^{\beta}. \tag{16.23}$$

By comparing this one-loop corrected theoretical result with experiment, one does find an improvement in the right direction.

The theory of critical indices has been the subject of many investigations in the past years. Therefore they deserve a more detailed discussion which will be given in a separate chapter. Let us end this section by pointing out that the appearance of an imaginary part for $\Phi^2 < \Phi_c^2$ has a good physical reason: Imaginary parts in an energy are always related to an instability of the system. The origin of the instability for $\Phi^2 < \Phi_c^2$ can easily be found: Let us turn on an external field j which drives Φ into the region of instability. The effective potential becomes

$$v(\Phi) = \frac{m^2}{2}\Phi^2 + \frac{g}{4!}\Phi^4 - j\Phi \tag{16.24}$$

and looks as plotted in Fig. 16.1.

The value of Φ at the minimum increases with j. The other minimum at the diametrally opposite place, however, begins to move closer to the axis. We can display the two minima as a function of j by plotting, in Fig. 16.3, the result Φ_j of the equation $\partial v(\Phi)/\partial\Phi = 0$: //[2em]

$$j = m^2\Phi + \frac{g}{3!}\Phi^3. \tag{16.25}$$

For very large j or $-j$, there is only a single minimum on the right- or left-hand side, respectively. In a region $|j| \leq j_c$ there are three solutions, two minima and one maximum. The value j_c is determined from the maximum of the curve (16.25)

$$j_c = -\sqrt{\frac{2m^2}{g}}\frac{2}{3}m^2 \tag{16.26}$$

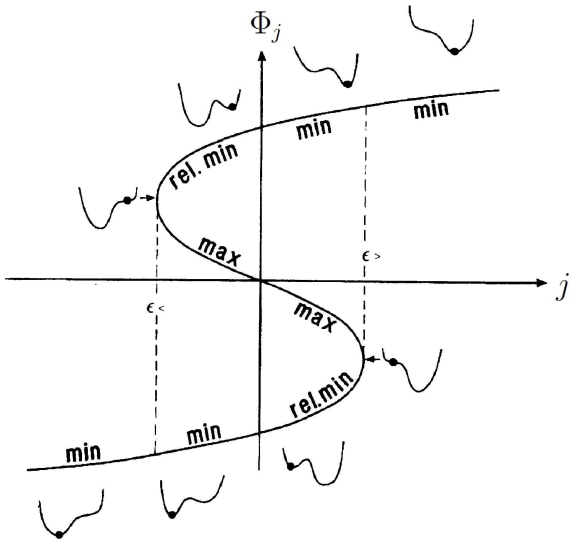

FIGURE 16.3 Magnetization Φ_j as a function of the external source j in mean-field approximation.

which lies at

$$\Phi_c^2 = -2m^2/g. \tag{16.27}$$

There the minimum fuses with the maximum and disappears. But this is precisely the place at which the effective potential develops an imaginary part. Thus the instability indicated by the appearance of an imaginary part in the effective potential is simply a signal for the fact that the local minimum at the elevated place can no longer be a solution of the field equation. The point becomes locally unstable. Note that the same instability point appears to all orders in the loop expansion, i.e., to all orders in the fluctuation expansion.

From our knowledge of simple quantum mechanical systems we may conclude that this result cannot contain the whole truth about phase stability. While the system certainly can be in the higher minimum, it always has a possibility of escaping through the potential barrier via tunneling. Thus there must be an imaginary part in the true effective potential as soon as $\Phi < \Phi^0$. Obviously, the loop expansion cannot account for this. Even the hope is futile that a full summation of all terms might produce a corresponding singularity at $\Phi = \Phi^0$. From quantum mechanics it is known that tunneling amplitudes carry an exponentially small suppression factor $e^{-a/g\hbar}$. Such a factor can never be derived from a loop expansion that is always a power series in g (the power series expansion of $e^{-a/g\hbar}$ would be $1 + 0 + 0 + \ldots$). Note however, that approximate methods have been developed to describe physical effects of this type. They are based on variational perturbation theory (VPT) that will be described in Section 22.5.

16.2 Nambu-Goldstone Particles

16.2.1 The Mechanism

There is an important physical consequence of spontaneous symmetry breakdown. The system has an infinite choice between different directions of ϕ. Consider a field configuration which is not constant in space but changes smoothly from space-time point to space-time point along the degenerate O(N) shell. Obviously, the energy of such a configuration can be made arbitrarily small. But this means that there is a large region in field space over which fluctuations hardly change the action. Thus the suppression of fluctuation cannot be very effective and the angular fluctuations of the field are large. Let us see this explicitly for the case $N = 2$ for which ϕ may be written as a single complex field $\phi = \phi_1 + i\phi_2$. Going to a radial decomposition

$$\phi = \rho e^{i\gamma}, \tag{16.28}$$

we may write the action as

$$\mathcal{A}[\phi] = \frac{1}{2}\left(\partial\rho\right)^2 - \frac{m^2}{2}\rho^2 + \frac{1}{2}\rho^2\left(\partial\gamma\right)^2 - \frac{g}{4}\rho^4. \tag{16.29}$$

For $m^2 < 0$, consider variations of ρ around $\rho_0 = \sqrt{-m^2/g}$. If $\gamma(\mathbf{x})$ is kept constant we may expand $\rho = \rho_0 + \delta\rho$ and write

$$\delta^2\mathcal{A}[\phi] = \frac{1}{2}\left(\partial\delta\rho\right)^2 + \frac{2m^2}{2}\left(\delta\rho\right)^2. \tag{16.30}$$

Note that the size fluctuations $\delta\rho$ take place with a mass twice the opposite of the $T > T_c^{\mathrm{MF}}$ situation. An O(2)-symmetric field theory with ϕ^4-interaction can be used to describe the phase transition from normal to superfluid in liquid helium near 2.7 degrees Kelvin. The O(2)-degeneracy of the ground state manifests itself by the independence of the action on γ. If γ has small space-time variations, we may write $\gamma = \gamma_0 + \delta\gamma$, and we get from the gradient term in (16.29) an additional piece in the action

$$\delta^2\mathcal{A}[\phi] = \frac{1}{2}{\rho_0}^2\left(\partial\delta\gamma\right)^2. \tag{16.31}$$

Consider now the eigenmodes of quadratic fluctuations. There is one mode associated with the size ρ of the field. From (16.30) we read off the propagator

$$G_{\delta\rho\delta\rho} = \frac{i}{-\partial^2 + 2m^2}. \tag{16.32}$$

The other fluctuation in the phase γ is seen from (16.31) to have a propagator

$$G_{\delta\gamma\delta\gamma} = \frac{1}{{\rho_0}^2}\frac{i}{-\partial^2}. \tag{16.33}$$

This is a massless mode, the famous *Nambu-Goldstone boson*. Its presence in the case of spontaneously broken symmetry was first discovered by Nambu, followed by a more rigorous treatment by Goldstone. If the action depends on an N-component vector field ϕ_a in an O(N)-symmetric way, there are $N-1$ Nambu-Goldstone bosons carried by the directional fluctuations $\delta\phi^0$ transverse to the direction Φ^0 of the ground state.

Remember that the physical origin is the arbitrarily small change of action for smooth continuous variations of the ground state directions.

At long distances, the only experimental correlations come from the massless modes. There exist many physical phenomena which are dominated by these. They can be studied approximately by ignoring completely the variations of the size of the field ρ, freezing it at the equilibrium value ρ_0. This is called the *hydrodynamic limit* of the field theory. It describes only the Nambu-Goldstone boson. In the O(N)-symmetric theory, the freezing of the size of the field leaves the directional vector $n_a = \phi_a/|\phi|$ free to fluctuate. Then the field theory model goes over into the classical Heisenberg model.

This limit will be discussed further in Section 19.2.

16.2.2 General Considerations

The necessity of a Nambu-Goldstone particle as a consequence of spontaneous symmetry breakdown can easily be proved for any continuous symmetry and to all orders in perturbation theory by using the full effective action. Let us look only at the case of O(N)-symmetry. The infinitesimal symmetry transformations on the currents are

$$j_a \to j_a - i\epsilon_{cd}\,(L_{cd})_{ab}\,j_b \tag{16.34}$$

where L_{cd} are the $N(N-1)/2$ generators of O(N)-rotations. Under this, the generating functional is invariant

$$\delta W[j] = \int dx \frac{\delta W[j]}{\delta j_a(x)} i\,(L_{cd})_{ab}\,j_b\epsilon_{cd} = 0. \tag{16.35}$$

Let us insert the Legendre transformation laws for Φ and j. Then (16.35) amounts to

$$0 = \int dx \Phi_a(x) i\,(L_{cd})_{ab}\,\frac{\delta\Gamma[\Phi]}{\delta\Phi_b(x)}\epsilon_{cd}\,, \tag{16.36}$$

which expresses the infinitesimal invariance of the effective action under

$$\Phi_a \to \Phi_a - i\epsilon_{cd}\,(L_{cd})_{ab}\,\Phi_b.$$

The invariance law (16.36) is often called the *Ward-Takahashi identity* for the functional $\Gamma[\Phi]$. It can be used to find an infinite set of identities with this name for all vertex functions by forming higher functional derivatives and setting $\Phi = \Phi^0$ at the

end. For example, the first derivative of (16.36) gives (dropping the infinitesimal parameter ϵ_{cd})

$$0 = (L_{cd})_{ab} \frac{\delta\Gamma[\Phi]}{\delta\Phi_b(x)} + \int dx' \Phi_{a'}(x') (L_{cd})_{a'b} \frac{\delta^2\Gamma[\Phi]}{\delta\Phi_b(x')\delta\Phi_a(x)}. \tag{16.37}$$

Setting $\Phi = \Phi^0$, where $j_a = \delta\Gamma[\Phi]/\delta\Phi_b(x) = 0$, gives

$$\int dx' \Phi^0_{a'}(x) (L_{cd})_{a'b} \frac{\delta^2\Gamma[\Phi^0]}{\delta\Phi^0_b(x')\delta\Phi^0_a(x)}.$$

At $\Phi = \Phi^0$, the second derivative of $\Gamma[\Phi^0]$ is simply the vertex function $\Gamma^{(2)}$ at zero momentum which equals the inverse of the connected two-point function in momentum space $G_c(p)$, due to Eq. (13.45). Hence we obtain

$$\Phi^0_{a'} (L_{cd})_{a'b} [G_c^{-1}]_{ba}(q = 0) = 0. \tag{16.38}$$

This statement implies that certain fully interacting propagators have to contain a singularity at $q = 0$. In most cases this is caused by a pole in the momentum square variable q^2. Then (16.38) implies the existence of a massless particle state in Hilbert space, the Nambu-Goldstone boson. We shall see later which exceptions are possible.

We have argued before that the directions of massless fluctuations must be associated with the valley of degenerate states in the effective potential. The above equation (16.38) is a mathematical expression of this conclusion.

As an example consider the case $N = 2$. Then $(L_{cd}\epsilon_{cd})_{ab}$ is simply the 2×2-matrix

$$\begin{pmatrix} 0 & -1 \\ 1 & 0 \end{pmatrix} \epsilon_{12}\,.$$

Let the vacuum expectation of the two-component field $\phi_a(x)$ be

$$\Phi^0 = \left(\Phi^0, 0\right).$$

Then (16.38) states that

$$[G_c^{-1}]_{22} (q = 0) = 0, \tag{16.39}$$

calling for a massless mode along the second field direction. Translating this into the complex field language studied previously, we rewrite $\Phi_a = (\rho\cos\gamma,\ \rho\sin\gamma)$ as

$$\Phi = \rho e^{i\gamma}.$$

For ρ close to ρ_0 and small γ, this is precisely the massless mode in the azimuthal variable.

For $N = 3$, the rotations may be written as

$$(L_{cd}\epsilon_{cd})_{ab} = -\epsilon_{dab}\alpha_d,$$

where α is a small angle of rotation and $\epsilon_{123} = 1$. Then (16.38) becomes

$$\epsilon_{abd}\Phi_a^0[G_c^{-1}]_{bc}(q=0) = 0. \tag{16.40}$$

If Φ_a^0 points into the direction of the third axis of the O(3)-sphere, the transverse modes $[G_c]_{11}^{(2)}$ and $[G_c]_{22}^{(2)}$ are massless.

Note that only statements on diagonal elements are non-trivial, since $[G_c^{(2)}]_{ij}$ vanishes unless $i = j$, as is obvious at the one-loop level and can be shown to hold for any invariant power $(\Phi_a^2)^n$ appearing in the effective action.

The Nambu-Goldstone theorem has an important exception if the field theory possesses a massless gauge boson from the outset. This is the case in a superconductor, where the electrons are coupled to an electromagnetic field. When a material is cooled below the transition temperature at which its resistance drops to zero, it also expels the magnetic field. This is called the Meissner-Ochsenfeld effect, discovered in 1933.[1] This effect constitutes the basis of present theories of weak interactions. It therefore deserves being discussed in detail in Chapters 17 and 27.

16.2.3 Experimental Consequences

The Nambu-Goldstone phenomenon has important observational consequences. The most simple experiment which can be done on a system is to study the change of energy as a function of an external field j. The functional derivative

$$\frac{\delta W[j]}{\delta j} = \langle 0|\phi(x)|0\rangle_{j=\text{const}} = \Phi \tag{16.41}$$

is observable directly as an order parameter of the system (say as a magnetization). The change of this order parameter with respect to changes in j is measured as the susceptibility $\chi(x, y)$:

$$\frac{\delta\Phi(x)}{\delta j(y)} = \frac{\delta^2 W[j]}{\delta j(x)\delta j(y)} = \langle 0|T\phi(x)\phi(y)|0\rangle \equiv \chi(x, y). \tag{16.42}$$

Its Fourier transform

$$(2\pi)^4\delta^{(4)}(q+q')\chi(q) = \int d^4x \int d^4x' e^{i(qx+q'x')}\chi(x, x') \tag{16.43}$$

at $q_0 = 0$ is called the static susceptibility. Using the identity (13.42), we may write equivalently

$$(2\pi)^4\delta^{(4)}(q+q')\chi^{-1}(q) = -\frac{\delta^2\Gamma[\Phi]}{\delta\Phi_a(q)\delta\Phi_b(q')}, \tag{16.44}$$

[1] W. Meissner and R. Ochsenfeld, Naturwissenschaften *21*, 787 (1933).

or

$$\chi^{-1}(0) = \frac{\partial^2 v}{\partial\Phi_a \partial\Phi_b}. \tag{16.45}$$

Let us calculate these quantities at the mean-field level. For $\tau > 0$ we find

$$\begin{aligned} \chi^{-1}_{ab}(q) &= \left(m^2 + \mathbf{q}^2 - q_0^2\right)\delta_{ab} = \left(\mu^2\tau + \mathbf{q}^2 - q_0^2\right)\delta_{ab}\,, \\ \chi^{-1}_{ab}(0) &= m^2\delta_{ab} = \mu^2\tau\delta_{ab}\,. \end{aligned} \tag{16.46}$$

Thus χ^{-1} increases linearly with τ. It is a favorite quantity for experimental plots. Very close to a critical point, the measurements show deviations from this law due to fluctuations. Near $T = T_c^{\rm MF}$, one measures a power law parametrized by

$$\chi^{-1}_{ab} = \mu^2\tau^\gamma\delta_{ab}.$$

The value of γ is called the *critical index* of susceptibility above $T_c^{\rm MF}$. The derivation of this power behavior will be given in Subsec. 20.9 [see Eq. (20.152)].

As the temperature passes below $T_c^{\rm MF}$, the spontaneous breakdown of O(N) symmetry leads to a drastic change: The susceptibility $\chi_{ab}(q)$ looses its isotropy in field space. The component $\chi_\parallel^{-1}(q)$ longitudinally to the direction Φ_a^0 is produced by the longitudinal projection matrix $(P_\parallel)_{ab} \equiv \Phi_a^0\Phi_b^0/(\Phi^0)^2$ and behaves like

$$\begin{aligned} \chi_\parallel^{-1}(q) &= -2m^2 + q^2 - q_0^2 = -2\mu^2\tau + q^2 - q_0^2, \quad \tau < 0, \\ \chi_\parallel^{-1}(0) &= -2m^2 = -2\mu^2\tau, \qquad\qquad\qquad\quad \tau < 0. \end{aligned} \tag{16.47}$$

Then N transverse components of χ^{-1}_{ab}, on the other hand, are obtained from the transverse projection matrix $(P_\perp)_{ab} \equiv \delta_{ab} - (P_\parallel)_{ab}$. They vanish at $q = 0$:

$$\chi_\perp^{-1}(q) = G^{-1}(q) = q^2 - q_0^2. \tag{16.48}$$

Thus $\chi_\perp$ diverges for $q \to 0$, and this leads to a dramatic experimental effect: If the external source describes incoming waves with weak space-time dependence, the system scatters these very strongly. For example, if j corresponds to an electromagnetic field in the optical range (as is the case in nematic liquid crystals), the system becomes completely opaque (it looks milky). When cooling through $T_c^{\rm MF}$, this phenomenon is called *critical opalescence*.

Note that a spontaneously broken *continuous* symmetry is necessary for the opalescence below $T_c^{\rm MF}$. In the case of a single real ϕ field (Ising-like system) there are no Goldstone modes and there is no $\chi_\perp^{-1}$ which stays identically equal to zero for $T < T_c^{\rm MF}$, $q = 0$. There, one sees critical opalescence just in the immediate vicinity of $T_c^{\rm MF}$, and the system becomes again clear below $T_c^{\rm MF}$.

16.3 Domain Walls in the O(1)-Symmetric Theory

The field equations following from the Lagrangian (16.1) are

$$\left[\partial^2 + m^2 + g\phi_b^2(x)\right]\phi_a(x) = 0. \tag{16.49}$$

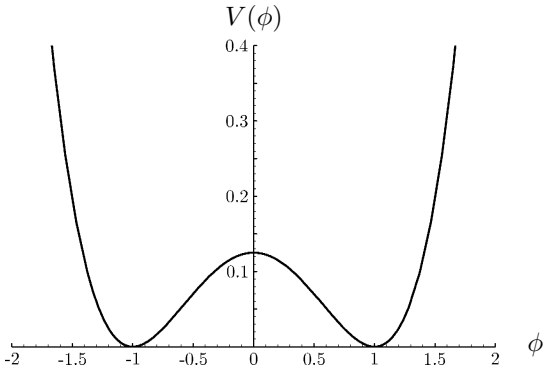

FIGURE 16.4 Plot of the symmetric double-well potential $V(x) = -\frac{1}{2}\phi^2 + \frac{1}{4}\phi^4$. We have added a trivial constant 1/4 to place the minima on the ϕ-axis.

For $m^2 < 0$, where the potential looks like the bottom of a champagne bottle in Fig. 16.1, these equations possess nontrivial static solutions solving the spatial part of the differential equation (16.49):

$$\left[-\boldsymbol{\nabla}^2 + m^2 + g\phi_b^2(\mathbf{x})\right]\phi_a(\mathbf{x}) = 0. \tag{16.50}$$

The simplest nontrivial solution varies only along one axis, say the x-axis, and only in one field component. It will turn out to be a stable solution only if the other components are absent altogether. There the Lagrangian (16.1) possesses merely a reflection symmetry $\phi \to -\phi$, which in the general context is called an O(1)-symmetry.

Thus we shall study the simplified field equation

$$\left[-\frac{d^2}{dx^2} + m^2 + g\phi^2(x)\right]\phi(x) = 0. \tag{16.51}$$

For a single field component, the potential has the form of a double-well pictured in Fig. 16.4. The equation (16.51) has two trivial constant solutions

$$\phi(x) \equiv \pm\phi_0 \equiv \sqrt{\frac{-m^2}{g}} \tag{16.52}$$

which lie at the two minima of the potential

$$V(\phi) = \frac{m^2}{2}V(x) = \frac{m^2}{2}\phi^2 + \frac{g}{4}\phi^4. \tag{16.53}$$

At the minimum, the potential has the value

$$V_c = -\frac{m^4}{g}, \tag{16.54}$$

which is called the *condensation energy* of the field system. It will be convenient to subtract this from $V(\phi)$ and write the subtracted potential

$$V(\phi) = \frac{m^2}{8\phi_0^2}(\phi - \phi_0)^2(\phi + \phi_0)^2, \tag{16.55}$$

exhibiting more directly the symmetric minima at $\phi = \pm\phi_0$ (see Fig. 16.4). The coupling strength is

$$g = m^2/2\phi_0^2. \tag{16.56}$$

Near the minima, the potential looks approximately like a harmonic oscillator potential $V_\pm(\phi_0) = m^2(x \mp \phi_0)^2/2$:

$$V(\phi) = \frac{m^2}{2}(\phi \mp \phi_0)^2 \left(1 \pm \frac{\phi \mp \phi_0}{\phi_0} + \dots\right) \equiv V_\pm(\phi) + \Delta V_\pm(\phi) + \dots \ . \tag{16.57}$$

The height of the potential barrier at the center is

$$V_{\max} = \frac{(m\phi_0)^2}{8}. \tag{16.58}$$

In the limit $\phi_0 \to \infty$ at a fixed frequency m, the barrier height becomes infinite and the system decomposes into a sum of two independent harmonic-oscillator potentials widely separated from each other.

The nontrivial solution of the field equation connects the two trivial solutions (16.52) across the barrier. As we shall derive immediately, this reads

$$\phi(x) = \phi_{\rm cl}^{\pm}(x) \equiv \pm\phi_0 \tanh[m(x - x_0)/2], \tag{16.59}$$

with an arbitrary parameter x_0 specifying the point on the x-axis where the crossing takes place. The crossing takes place over a distance of the order of $2/m$. For large positive and negative x, the solution approaches $\pm\phi_0$ exponentially (see Fig. 16.5).

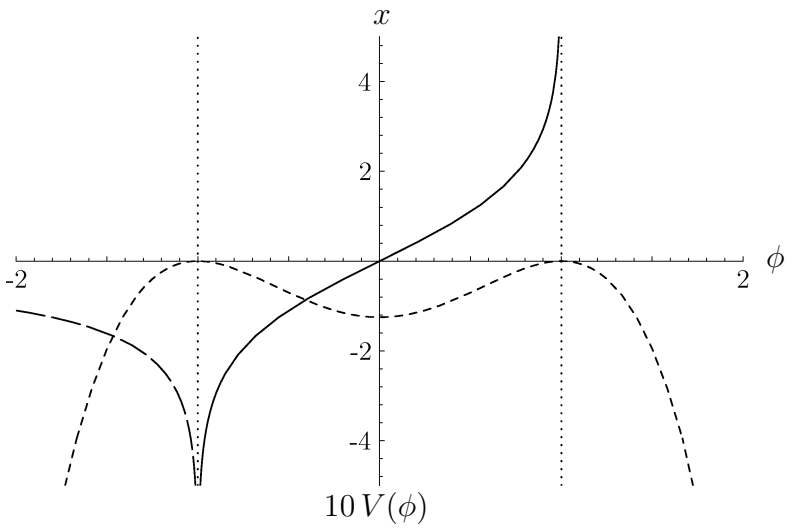

FIGURE 16.5 Classical kink solution (solid curve) in double-well potential (short-dashed curve with units marked on the lower half of the vertical axis). The solution connects the two degenerate maxima in the reversed potential. The long-dashed curve starts out at a maximum and slides down into the adjacent abyss.

The subscript cl on $\phi_{\rm cl}$ emphasized that these solutions solve the classical field equations. Alluding to their shape, the solutions $\phi^{\pm}_{\rm cl}(x)$ are called *kink* and *antikink* solutions, respectively.[2]

To derive these solutions, consider the equation of motion (16.51) in the pseudotime $t = ix$,

$$\ddot{\phi}(t) = -V'(\phi(t)), \tag{16.60}$$

where $V'(\phi) \equiv dV(\phi)/d\phi$). Since the differential equation is of second order, there is merely a sign change in front of the potential with respect to the spatial differential equation (16.51). The equation of motion (16.60) therefore corresponds to a usual equation of motion of a point particle as a function of the pseudotime t, whose potential is turned upside down with respect to Fig. 16.4. This is illustrated in Fig. 16.6. The reversed potential allows obviously a classical solution which starts

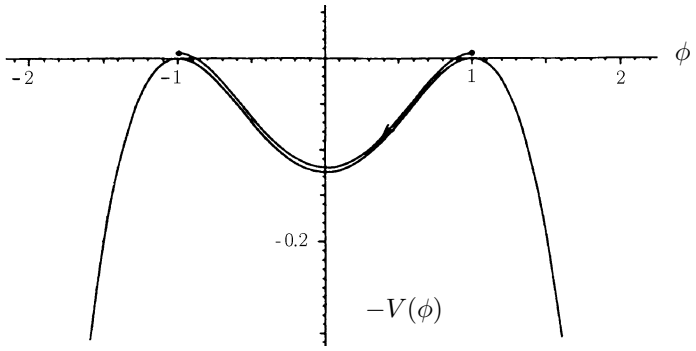

FIGURE 16.6 Reversed double-well potential governing the motion of the position ϕ as a function of the imaginary time x.

out at $\phi = -\phi_0$ for $x \to -\infty$ and arrives at $\phi = \phi_0$ for $x \to +\infty$. The particle needs an infinite time to leave the initial potential mountain and to climb up to the top of the final one. The movement through the central valley proceeds within the finite time $\approx 2/m$. If the particle does not start its movement exactly at the top but slightly displaced towards the valley, say at $\phi = -a + \epsilon$, it will reach $\phi = a - \epsilon$ after a finite time, then return to $\phi = -a + \epsilon$, and oscillate back and forth forever. In the limit $\epsilon \to 0$, the period of oscillation goes to infinity and only a single crossing of the valley remains.

To calculate this movement, the differential equation (16.49) is integrated once after multiplying it by $\phi' = dx/dx$ and rewriting it as

$$\frac{1}{2}\frac{d}{dx}x'^2 = \frac{d}{dx}V(\phi(x)). \tag{16.61}$$

[2]In much of the the field-theoretic literature, such solutions are also referred to as *instanton* or *anti-instanton* solutions, the name emphasizing the fact that the valley is crossed within a short time interval. See the references quoted at the end of the chapter.

The integration gives

$$\frac{x'^2}{2} + [-V(\phi(x))] = \text{const}\,. \tag{16.62}$$

If x is reinterpreted as the physical time, this is the law of *energy conservation* for motion in the reversed potential $-V(\phi)$. Thus we identify the integration constant in (16.62) as the total energy E in the reversed potential:

$$\text{const} \equiv E. \tag{16.63}$$

Integrating (16.62) further gives

$$x - x_0 = \pm\frac{1}{\sqrt{2}} \int_{\phi(x_0)}^{\phi(x)} \frac{d\phi}{\sqrt{E + V(\phi)}}. \tag{16.64}$$

A look at the potential in Fig. 16.6 shows that an orbit that starts out with the particle at rest for $x \to -\infty$ must have $E = 0$. Inserting the explicit potential (16.55) into (16.64), we obtain for $|\phi| < \phi_0$

$$\begin{aligned} x - x_0 &= \pm\frac{2phi_0}{m} \int_0^{\phi} \frac{d\phi'}{(\phi_0 - \phi')(\phi' + \phi_0)} = \pm\frac{1}{m}\log\frac{\phi_0 + \phi}{\phi_0 - \phi} \\ &= \pm\frac{2}{m}\text{artanh}\frac{\phi}{\phi_0}. \end{aligned} \tag{16.65}$$

Thus we find the kink and antikink solution (16.59) crossing the barrier.

The euclidean action of such a solution can be calculated as follows [using (16.62) and (16.63)]:

$$\begin{aligned} \mathcal{A}_{\text{cl}} &= \int_{-\infty}^{\infty} dx \left[\frac{{\phi'_{\text{cl}}}^2}{2} + V(\phi_{\text{cl}}(x))\right] = \int_{-\infty}^{\infty} dx({\phi'}^2_{\text{cl}} - E) \\ &= -EL + \int_{-a}^{a} dx\sqrt{2[E + V(\phi)]}. \end{aligned} \tag{16.66}$$

The kink has $E = 0$, so that

$$\sqrt{2(E + V(\phi))} = \frac{m}{2\phi_0}(\phi_0^2 - \phi^2), \tag{16.67}$$

and the classical action becomes

$$\mathcal{A}_{\text{cl}} = \frac{m}{2\phi_0} \int_{-\phi_0}^{\phi_0} d\phi(\phi_0^2 - \phi^2) = \frac{2}{3}\phi_0^2 m = \frac{m^3}{3g}. \tag{16.68}$$

Note that for $E = 0$, the classical action is also given by the integral

$$\mathcal{A}_{\text{cl}} = \int_{-\infty}^{\infty} dx\ \frac{{\phi'_{\text{cl}}}^2}{2}. \tag{16.69}$$

There are also solutions starting out at the top of either mountain and sliding down into the adjacent exterior abyss, for instance (see again Fig. 16.6)

$$\begin{aligned} x - x_0 &= \mp\frac{2\phi_0}{m}\int_\phi^\infty \frac{d\phi'}{(\phi'-\phi_0)(\phi'+\phi_0)} = \pm\frac{1}{m}\log\frac{\phi+\phi_0}{\phi-\phi_0} \\ &= \pm\frac{2}{m}\text{arcoth}\frac{\phi}{\phi_0}. \end{aligned} \tag{16.70}$$

However, these solutions cannot connect the bottoms of the double well with each other and will not be considered further.

The real ϕ^4-theory can be used as a model for a spin system, in which the spins can point only in two directions. In statistical mechanics, such a system is usually described by the *Ising model* on a lattice. In fact, it can be shown that the Ising model can be transformed into a real ϕ^4-field theory whose potential can be approximated, near the phase transition, by a ϕ^4-potential. The two spin directions are represented in the ϕ^4-theory by the two minima of the potential. The classical solution to the field equation may be interpreted as a domain wall between up and down directions. Domain walls can occur in many possible shapes which are too hard to calculate analytically. They possess a high configurational entropy, and the demagnetization transition can be understood as a transition in the ensemble of fluctuating domain walls of any shape. Their configurational entropy overcomes the energy consumed in the process of creating the domain walls.

Let us finally realize that domain walls in O(N)-symmetric theories cannot be stable: It is always possible to rotate the spin direction of one domain into another direction thereby lowering continuously the energy. This is impossible for a single-component real ϕ-field.

16.4 Vortex Lines in the O(2)-Symmetric Theory

The most important domain of application of the O(2)-symmetric theory is the study of the superfluid phase transition in liquid helium at $T_c \approx 2.3\,\text{K}$. The two-component ϕ^4 theory is then referred to as *Landau-Pitaevskii theory*. Its euclidean action is written in terms of a complex field $\varphi = (\phi_1 + i\phi_2)/\sqrt{2}$ in $D = 3$ space dimensions as an energy density

$$\mathcal{H} = \varphi^*(\mathbf{x})\left(-\frac{\hbar^2}{2M}\boldsymbol{\nabla}^2 - \mu\right)\varphi(\mathbf{x}) + g|\varphi(\mathbf{x})|^4, \tag{16.71}$$

where μ is the chemical potential which passes through zero at some critical mean-field temperature T_c^{MF}:

$$\mu = \mu_0\left(\frac{T}{T_c^{\text{MF}}} - 1\right). \tag{16.72}$$

The quartic term approximates the repulsion between the helium atoms by a δ-function potential [recall the second-quantized Hamiltonian (2.139)].

The field equation which minimizes this energy density is

$$\left(-\frac{\hbar^2}{2M}\boldsymbol{\nabla}^2 - \mu + g|\varphi|^2\right)\varphi = 0. \tag{16.73}$$

It possesses cylindrical solutions which are observable in the laboratory in the form of straight vortex lines. To find these, we decompose φ into its polar components as $\varphi = \rho e^{i\gamma}$, and find from the real and imaginary parts of Eq. (16.73) the two equations

$$\left\{-\frac{\hbar^2}{2M}\left[\boldsymbol{\nabla}^2 - (\boldsymbol{\nabla}\gamma)^2\right] - \mu + g\rho^2\right\}\rho = 0, \tag{16.74}$$

and

$$\boldsymbol{\nabla}(\rho^2\boldsymbol{\nabla}\gamma) = 0. \tag{16.75}$$

The latter equation is simply the radial-azimuthal form of the conservation law for the particle current $\mathbf{j}$:

$$\boldsymbol{\nabla}\,\mathbf{j} = \boldsymbol{\nabla}\left(\frac{1}{2i}\varphi^*\overset{\leftrightarrow}{\boldsymbol{\nabla}}\varphi\right) = 0. \tag{16.76}$$

Equation (16.75) can be solved by a purely circular flow of particles, in which ρ depends on the spatial distance r from the cylindrical axis, and the phase γ of the complex field is an integer multiple of the azimuthal angle in space, $\theta \equiv \tan^{-1}(x_2/x_1)$, i.e.,

$$\gamma = n\theta. \tag{16.77}$$

Then, (16.74) reduces to the radial differential equation

$$-\frac{\hbar^2}{2M}\left(\partial_r^2 + \frac{1}{r} - \frac{n^2}{2}\right)\rho + g(\rho^2 - \rho_0^2)\rho = 0, \tag{16.78}$$

where $\rho_0 = |\varphi_0| = \sqrt{-\mu/g} = \sqrt{-\mu_0(T/T_c^{\rm MF} - 1)/g}$ [compare (16.73)].

In order to solve Eq. (16.78), it is convenient to go to the reduced quantities

$$\bar{x} \equiv x/\xi, \qquad \bar{r} \equiv r/\xi, \tag{16.79}$$

which measure the distances in units of the coherence length

$$\xi = \sqrt{2}\xi_{\rm size} = \sqrt{\frac{\hbar^2}{2Mg\varphi_0^2}} = \sqrt{\frac{\hbar^2}{2M}\frac{1}{(-\mu_0)}}\sqrt{\frac{T}{T_c^{\rm MF}} - 1}^{-1}. \tag{16.80}$$

We also measure the size of the order parameter ρ in units of ρ_0, and introduce the reduced field strength

$$\bar{\rho} \equiv \rho/\rho_0 = |\varphi|/|\varphi_0. \tag{16.81}$$

Then (16.78) takes the form

$$\left[-\left(\partial_{\bar{r}}^2 + \frac{1}{\bar{r}}\partial_{\bar{r}} - \frac{n^2}{\bar{r}^2}\right) + (\bar{\rho}^2 - 1)\right]\bar{\rho}(\bar{r}) = 0. \tag{16.82}$$

For small $\bar{r} \ll 1$, this is dominated by the terms in the first parentheses, leading to a differential equation of the Bessel type for $\bar{\rho}(\bar{r})$. Thus, close to the origin, the solution is

$$\bar{\rho}(\bar{r}) = A_n J_n(\bar{r}) \propto \bar{r}^n, \tag{16.83}$$

where $J_n(\bar{r})$ is the standard Bessel function. Multiplying this with the phase factor

$$e^{in\gamma} = e^{in\tan^{-1}(x_2/x_1)}, \tag{16.84}$$

we see that the complex field $\varphi(x)$ has the following small-$|\mathbf{x}|$ behavior:

$$\varphi(\mathbf{x}) \propto \bar{r}^n e^{in\tan^{-1}(x_2/x_1)} = (x_1 + ix_2)^n, \tag{16.85}$$

exhibiting a zero of n-th order in the complex plane $x_1 + ix_2$.

For large $\bar{r} \gg 1$, $\bar{\rho}(\bar{r})$ approaches the asymptotic value $\bar{\rho} = 1$. In fact, from (1.44) we can extract the $1/\bar{r}$ expansion,

$$\bar{\rho}_n(\bar{r}) = 1 - \frac{n^2}{2\bar{r}^2} - \left(n^2 + \frac{1}{8}n^4\right)\frac{1}{\bar{r}^4} - \left(8 + 2n^2 + \frac{1}{16}n^4\right)\frac{n}{\bar{r}^6} - O\left(\frac{1}{\bar{r}^8}\right). \tag{16.86}$$

Integrating the differential equation numerically inward, we find the solution displayed in Fig. 16.7. What is the energy of these vortex lines? In order to find a

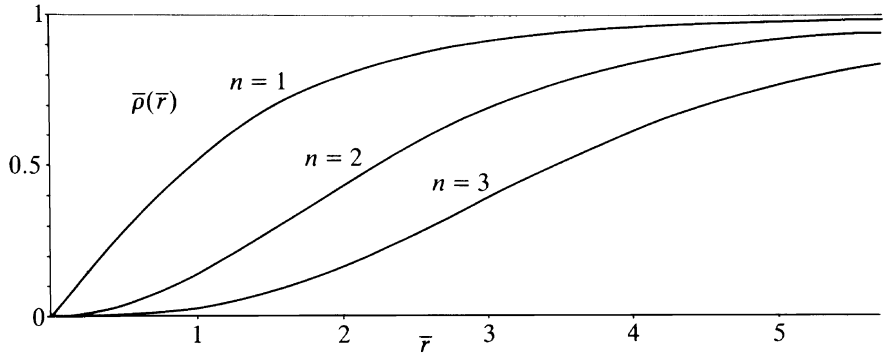

FIGURE 16.7 Reduced order parameter $\bar{\rho} = |\varphi|/|\varphi_0|$ around a vortex line of strength $n = 1, 2, 3, \ldots$ as a function of the reduced distance $\bar{r} = r/\xi$, where r is the distance from the axis and ξ the healing length.

convenient expression for it we use the fact that, if $\varphi(\mathbf{x})$ is a solution of the differential equation (16.73), the rescaled solution

$$\varphi_\delta(\mathbf{x}) \equiv e^\delta \varphi(\mathbf{x}) \tag{16.87}$$

must extremize the energy as a function of δ at $\delta = 0$. In terms of the reduced quantities of Eqs. (16.79) and (16.81), the energy is given by

$$E = E_c \int d^3\bar{x} \left[|\overline{\boldsymbol{\nabla}}\bar{\varphi}|^2 - |\bar{\varphi}|^2 + |\bar{\varphi}|^4\right], \tag{16.88}$$

where

$$E_c = \frac{\mu^2}{4g} \tag{16.89}$$

is the condensation energy. Inserting the reduced version of (16.87) into (16.88), we obtain

$$E = E_c \int d^3\bar{x} \left[e^{2\delta} |\overline{\boldsymbol{\nabla}} \bar{\varphi}|^2 - e^{2\delta} |\bar{\varphi}|^2 + e^{4\delta} |\bar{\varphi}|^4 \right]. \tag{16.90}$$

Setting the derivative with respect to δ equal to zero gives, at $\delta = 0$,

$$E_c \int d^3\bar{x} \left[|\overline{\boldsymbol{\nabla}} \bar{\varphi}|^2 - |\bar{\varphi}|^2 + 2|\bar{\varphi}|^4 \right] = 0. \tag{16.91}$$

Subtracting this from (16.90) at $\delta = 0$, we find that the energy of a solution of the field equation is simply given by

$$E = -E_c \int d^3\bar{x} |\bar{\varphi}|^4. \tag{16.92}$$

Most of this energy is due to the asymptotic value $|\bar{\varphi}| \to 1$, where E is equal to the negative condensation energy $-E_c$. Subtracting this from (16.90) at $\delta = 0$, we find the *additional energy* of the vortex line as

$$E_v = E_c \int d^3x (1 - |\bar{\varphi}|^4). \tag{16.93}$$

Going over to cylindrical coordinates $\bar{r}, \theta, z$, the integral becomes, for a vortex line of length L along the z-direction:

$$E_v = E_c \, 2\pi \bar{L} \int_0^x d\bar{r}\bar{r} \left[1 - \bar{\rho}^4(\bar{r}) \right]. \tag{16.94}$$

Before inserting the numerical solutions for $\bar{\rho}(\bar{r})$ shown in Fig. (16.7), we note that due to the factor $\bar{r}$, the additional energy comes mainly from the large $\bar{r}$ regime, i.e., from the far zone. In fact, if we insert the leading asymptotic behavior (16.86), we obtain an integral

$$E_v = E_c \, 4\pi n^2 \bar{L} \int^\infty \frac{d\bar{r}}{\bar{r}}, \tag{16.95}$$

which diverges logarithmically for large $\bar{r}$. An immediate conclusion is that a single vortex line can have a finite energy only in a container of finite size. In a cylindrical container of finite length L and finite radius R, the r-integral no longer diverges, and we obtain

$$E_v = E_c \, 4\pi n^2 \bar{L} \log(R/\xi). \tag{16.96}$$

Consider now the energy in the small-$\bar{r}$ regime, where Eq. (16.83) tells us that $\bar{\rho}(\bar{r})$ behaves like $\bar{r}^n$. Hence, $1 - \bar{\rho}^4 \approx 1$, and the energy of a thin cylindrical section of

radius r grows like r^2. For increasing r, the rate of growth slows down rapidly and settles at the asymptotic rate $4\pi n^2 L \times \log(\bar{r}/\xi)$, where ξ is the coherence length. The proper inclusion of the non-asymptotic behavior gives simply a finite correction to the asymptotic energy, and the energy of a vortex line in a container of radius R becomes

$$E_v = E_c\, 4\pi n^2 \bar{L}[\log(R/\xi) + c]. \tag{16.97}$$

This is the same result that would have been obtained by replacing in (16.94) the integrand $\bar{r}[1 - \bar{\rho}^4(\bar{r})]$ by the asymptotic form $2n^2/\bar{r}$, and performing the integral from the radius $r_0 = \xi e^{-c}$ to R.

The precise numerical evaluation of the differential equation (16.82) and the integral (16.94) shows that for the lowest vortex line, c has the value

$$c = 0.385. \tag{16.98}$$

Hence the energy of the vortex line becomes

$$E_v = E_c \bar{L}\, 4\pi n^2 [\log(R/\xi) + 0.385]. \tag{16.99}$$

The logarithmic divergence of the energy has a simple physical origin. In order to see this, let us calculate the energy once more in another way, using the original expression (16.88), i.e. without invoking the virial theorem. It reads, for the radial solutions,

$$E_v = E_c\, 4\pi \bar{L} \int d\bar{r}\bar{r} \left[(\partial_{\bar{r}} \bar{\rho})^2 + \frac{1}{2}(1 - \bar{\rho}^2)^2 + \frac{n^2}{\bar{r}^2}\bar{\rho}^2 \right]. \tag{16.100}$$

The first two terms are rapidly convergent. Thus the energy of the far zone resides completely in the last term

$$\frac{n^2}{\bar{r}^2}\bar{\rho}^2 \approx \frac{n^2}{\bar{r}^2}. \tag{16.101}$$

This energy is a consequence of the angular behavior of the condensate phase $\gamma = n \tan^{-1}(x_2/x_1)$ around a vortex line. It comes entirely from the *azimuthal part* of the gradient energy $(\hbar^2/2M^2)|\varphi|^2(\boldsymbol{\nabla}\gamma)^2$, i.e., the term which describes the *Nambu-Goldstone modes*. This is not surprising. We have discussed before that the *long range properties* of the system are dominated by these modes. A phase of the field φ which behaves like $\gamma = n \tan^{-1}(x_2/x_1)$ can be viewed as a coherent pile-up of these modes determining the energy in the far zone.

The dominance of the energy carried by the phase gradient can also be described in a different and more physical way. In the last section we identified the gradient $(\hbar/M)\boldsymbol{\nabla}\gamma$ with the superfluid velocity. For the vortex line at hand, the superfluid velocity is found, far away from the line, to be

$$\mathbf{v}_s = \frac{\hbar}{M} n \boldsymbol{\nabla} \tan^{-1}\left(\frac{x_2}{x_1}\right) = \frac{\hbar}{M}\frac{n}{r^2}(-x_2, x_1, 0) = \frac{\hbar}{M} n \frac{1}{r}\mathbf{e}\phi, \tag{16.102}$$

where $\mathbf{e}_\phi$ is the unit vector in the azimuthal direction. Thus, around every vortex line, there is a circular flow of the superfluid whose velocity decreases like the inverse distance from the line. The hydrodynamic energy density of this flow is

$$\mathcal{E}(\mathbf{x}) = \frac{\rho_s}{2}\mathbf{v}_s^2 = \frac{\rho_s}{2}\frac{\hbar^2}{M^2}\frac{n^2}{r^2}. \tag{16.103}$$

This is precisely the dominant third term in the energy integral (16.100). Thus the energy of the vortex line is indeed mainly due to the hydrodynamic energy of the superflow around the line. For a major part of the volume, the hydrodynamic limits in expression (16.103) give an excellent approximation. Only in the neighborhood of the line, i.e., for small radii $r \leq \xi$, the energy density differs from (16.103) due to gradients in the size of the field $|\varphi|$. It is therefore suggestive to idealize the superfluid and assume the validity of the pure gradient energy density

$$\mathcal{E}(\mathbf{x}) = \frac{\rho_s}{2}\mathbf{v}_s^2 = \frac{\sigma}{2}(\boldsymbol{\nabla}\gamma)^2, \quad \sigma \equiv \rho_s\frac{\hbar^2}{M^2}, \tag{16.104}$$

everywhere in space, where ρ_s is the *superfluid density*.

The deviations from this law, which become significant only very close to a vortex line, i.e., at distances of the order of the coherence length ξ, are treated approximately by simply cutting off the energy integration at a radius ξ away from a vortex line. In other words, we pretend as though there is no superflow at all within the thin tubes of radius ξ, with a sudden onset of idealized flow outside ξ, moving with the limiting velocity (16.102).

Although the internal part of the thin tube carries no superflow, it does carry rotational energy. Within the present approximation, this energy is associated with the number 0.385 in (16.99). This piece is called the *core energy*. The core energy has a physical interpretation. At distances smaller than the coherence length, the different parts of the liquid can no longer slip past each other freely. Hence the core of a vortex line is expected to rotate roughly like a solid rod, rather than with the diverging velocity $v_s \sim 1/r$. Indeed, if we use the approximation for a line of vortex strength n,

$$v_s \propto n \begin{cases} \dfrac{1}{r}, & r > \xi, \\ \dfrac{r}{\xi^2}, & r \leq \xi, \end{cases} \tag{16.105}$$

the energy density behaves like r^2, for small r, as observed before. Moreover, the energy integration gives

$$n^2\left[\int_1^{R/\xi} d\bar{r}/\bar{r} + \int_0^1 d\bar{r}\bar{r}^3\right] = n^2[\log(R/\xi) + 0.25], \tag{16.106}$$

and we see that the number for the core energy, 0.25, emerges with the right order of magnitude.

In order to complete our discussion of the hydrodynamic picture, let us calculate the circulation of the superfluid velocity field around the vortex lines:

$$\kappa \equiv \oint_B d\mathbf{x} \cdot \mathbf{v}_s = \frac{\hbar}{M} n \oint_B d\mathbf{x} \cdot \boldsymbol{\nabla}\gamma = \frac{\hbar}{M} 2\pi n = n\frac{h}{M} = n\kappa_1. \tag{16.107}$$

This integral is the same for any size and shape of the circuit B around the vortex line. Thus the circulation is quantized. It always appears in multiplets of $\kappa_1 = h/M \approx 10^{-3}$ cm^2/sec. The number n is called *vortex strength*.

The integral (16.107) can be transformed into a surface integral via Stokes' theorem:

$$\int_{S^B} d\mathbf{S} \cdot (\boldsymbol{\nabla} \times \mathbf{v}_s) = \frac{\hbar}{M} 2\pi n, \tag{16.108}$$

where S^B is some surface spanned by the circuit B in (16.107), and $d\mathbf{S}$ is the surface element. This integral is the same for any size and shape of S^B. From this result we conclude that the third component of the curl of $\mathbf{v}_s$ must vanish everywhere, except at the origin. There it must have a singularity of such a strength that the two-dimensional integral gives the correct vortex strength. Hence

$$\boldsymbol{\nabla} \times \mathbf{v}_s = \frac{\hbar}{M} 2\pi n \delta^{(2)}(\mathbf{x}_T)\hat{\mathbf{z}}, \tag{16.109}$$

where $\hat{\mathbf{z}}$ is the unit vector along the z-axis and $\mathbf{x}_T \equiv (x_1, x_2)$ are the coordinates orthogonal to the vortex line.

If the nonlinearities of the field equation are taken into account, the $\delta^{(2)}$-function is really smeared out over a circle whose radius is of order ξ. As an example, let us replace $1/r^2$ in (16.103) by $1/(r^2 + \varepsilon^2)$. Then the rotation of the superfluid velocity becomes

$$\boldsymbol{\nabla} \times \mathbf{v}_s = \frac{\hbar}{M} n \frac{2\varepsilon^2}{(r^2 + \varepsilon^2)^2} \hat{\mathbf{z}}. \tag{16.110}$$

The right-hand side is non-zero only within a small radius $r \neq \varepsilon$, where it diverges with the total strength

$$\int d^2x \frac{2\varepsilon^2}{(r^2 + \varepsilon^2)^2} = 2\pi\varepsilon^2 \int_0^\infty dr \frac{2r}{(r^2 + \varepsilon^2)^2} = 2\pi. \tag{16.111}$$

This shows that (16.110) is, indeed, a smeared out version of the δ-function relation (16.109).

Because of their rotational properties, vortex lines can be generated experimentally by rotating a vessel with an angular velocity m. Initially, the lack of friction will cause the superfluid part of the liquid to remain at rest. This situation cannot, however, persist forever since it is not in a state of thermal equilibrium. After some time, vortex lines form on the walls. They migrate into the liquid and distribute

themselves evenly. This goes on until their total number is such that the rotational Helmholtz free energy

$$F_\Omega = F - \Omega \cdot \mathbf{L} \approx \int d^3x \left(\frac{\rho_s}{2} \mathbf{v}_s^2 - \Omega \cdot \mathbf{x} \times \rho_s \mathbf{v}_s \right) \tag{16.112}$$

is minimal. This equilibration process has been observed in the laboratory and has even been photographed directly using the property that vortex lines trap ions which can be accelerated against a photographic plate. Integrating (16.112) with $\mathbf{v}_s$ from (16.102), we find that in a cylindrical vessel of radius R, the first vortex line $n = 1$ appears at a critical angular velocity

$$\Omega_c = \frac{\kappa_1}{\pi R^2} \log \frac{R}{\xi} \tag{16.113}$$

and settles on the axis of rotation.

Note that vortex lines of higher n are all unstable. Since the energy increases quadratically with n, it is favorable for a single line of higher n to decay into n lines of unit strength. When generating vortex lines by stirring a vessel, one may nevertheless be able to create, for a short time, such unstable lines, and observe their decay.

Notes and References

For more information on vortex lines see the review articles by
A.L. Fetter, *Quantum Theory of Superfluid Vortices*, Phys. Rev.**162**, 1437 (1967); *Rotating Trapped Bose-Einstein Condensates*, Rev. Mod. Phys. **81**, 647 (2009).
See also the textbook
H. Kleinert, *Gauge Fields in Condensed Matter*, Vol. I: *Superflow and Vortex Lines*, World Scientific, 1989 (`http://klnrt.de/b1`),
as well as:
H. Kleinert and V. Schulte-Frohlinde, *Critical Properties of ϕ^4-Theories*, World Scientific, Singapore 2001 (`http://klnrt.de/b8`);
H. Kleinert, *Multivalued Fields in Condensed Matter, Electromagnetism, and Gravitation*, World Scientific, Singapore 2009, pp. 1–497 (`http://klnrt.de/b11`).